

### Three-dimensional curved flames: Stationary flames in cylindrical tubes

V. V. Bychkov,<sup>1</sup> A. I. Kleev,<sup>2</sup> M. A. Liberman,<sup>2,3</sup> and S. M. Golberg<sup>3</sup>

<sup>1</sup>*Department of Plasma Physics, Umea University, S-90187, Umea, Sweden*

<sup>2</sup>*P. Kapitsa Institute for Physical Problems, 117334, Moscow, Russia*

<sup>3</sup>*Department of Physics, Uppsala University, Box 530, S-751 21, Uppsala, Sweden*

(Received 12 December 1996)

Curved axisymmetric stationary flames in cylindrical tubes are investigated on the basis of a model nonlinear equation for a flame front subject to the Landau-Darrieus instability. It is found that the increase of the flame velocity due to a curved shape of the front is much larger for the case of three-dimensional curved flames compared to the two-dimensional ones. Some of important properties of curved three-dimensional flames differ qualitatively from the properties of two-dimensional flames. Particularly, a regime of strong initiation of the Landau-Darrieus instability in narrow tubes is obtained, when all perturbation modes of small amplitudes are stable, but a curved stationary flame is still possible. Another important feature of the three-dimensional flame propagation is unlimited increase of the flame velocity with the increase of the tube diameter. [S1063-651X(97)51507-8]

PACS number(s): 82.40.Py, 47.20.-k

As it has been observed experimentally [1-3] and in two-dimensional (2D) simulations [4,5], premixed flame fronts in tubes usually acquire a curved shape instead of a more simple planar configuration. Quite often the curved flame shape is caused by the development of the hydrodynamic Landau-Darrieus (LD) instability of a flame front [1], which bends an initially planar front. It is well known [6-8], that on the linear stage of the LD instability small perturbations of a planar flame front grow exponentially  $\propto \exp(\sigma t + i\mathbf{k} \cdot \mathbf{x})$  with the instability growth rate  $\sigma$  depending on the perturbation wave number  $\mathbf{k}$  as

$$\sigma = S U_f (|\mathbf{k}| - k^2 \lambda_c / 2\pi), \quad (1)$$

where  $U_f$  is the velocity of a planar flame front, the coefficient  $S$  is a function of the ratio  $\Theta$  of the fuel density and the density of the burnt matter  $S = \Theta(\sqrt{\Theta + 1} - 1/\Theta - 1)/\Theta + 1$ . The growth of perturbations of a small amplitude is suppressed by thermal conduction, if a perturbation wavelength  $\lambda = 2\pi/|\mathbf{k}|$  is shorter than the cut-off wavelength  $\lambda < \lambda_c$ . As usual the cut-off wavelength exceeds the flame thickness considerably.

Propagation of curved flames resulting from the LD instability in initially uniform fuel mixtures is traditionally described by the model nonlinear equation [9-12]

$$\frac{\partial f}{\partial t} + \frac{\alpha(\Theta)}{2} U_f (\nabla f)^2 = S U_f \left( \hat{I}(f) + \frac{\lambda_c}{2\pi} \nabla^2 f \right), \quad (2)$$

where the shape of a curved flame front propagating along the  $z$  axis is given by  $z = f(\mathbf{x}, t) - U_f t$ . The integral operator  $\hat{I}$  in Eq. (2) is defined as

$$\hat{I}(f) = \frac{1}{4\pi^2} \int_{-\infty}^{\infty} |\mathbf{k}| f_k \exp(i\mathbf{k} \cdot \mathbf{x}) d\mathbf{k}, \quad (3)$$

where  $f_k$  is the Fourier transform of  $f$ . The linear terms in Eq. (2) give the dispersion relation of the LD instability of the planar flame front, Eq. (1), with the influence of small

but finite flame thickness described by the term proportional to the cut-off wavelength  $\lambda_c$ . The nonlinear term in Eq. (2) takes into account the interaction of modes of considerable amplitude. Originally, a nonlinear equation for a curved flame analogous to Eq. (2) has been derived in [9] for the complete set of hydrodynamic equations for a flame front, but the peculiar limit of a small expansion coefficient  $\Theta - 1 \ll 1$  (and almost planar flame shape) has been assumed in the derivation. In the original equation one has the coefficients  $S \approx \frac{1}{2}(\Theta - 1)$  and  $\alpha \approx 1$ . Since the paper [9] there has been always a problem how to extrapolate the results of the nonlinear equation depending strongly on the coefficient  $\alpha$  to the realistic case of large expansion coefficients  $\Theta = 5 - 10$ . The lack of a reliable estimate for  $\alpha$  made impossible the comparison of the results of Eq. (2) to results of experiments and direct numerical simulations.

To find the correct value of the coefficient  $\alpha$  in Eq. (2) we compare the analytical solution [10] of the 2D version of Eq. (2) and the results of the 2D numerical simulations of flame dynamics in a tube for the complete set of the hydrodynamical equations [5]. According to the analytical solution [10] the velocity  $U_w$  of a 2D curved stationary flame  $f(x, t) = F(x) - (U_w - U_f)t$  in a tube of width  $R$  with ideally slip and adiabatic walls may be written as

$$U_w = U_f + 4 U_m M \frac{\lambda_c}{2R} \left( 1 - M \frac{\lambda_c}{2R} \right), \quad (4)$$

where  $M = \text{Int}(R/\lambda_c + \frac{1}{2})$  and the maximal velocity increase is  $U_m = U_f S^2 / 2\alpha$ . Numerical simulations of flame dynamics in an ideal 2D tube for the case of realistic expansion coefficients  $\Theta = 5 - 10$  demonstrated the same dependence of the flame velocity on the tube width as given by Eq. (4) with the maximal velocity increase depending on the expansion coefficient as

$$U_m = \frac{U_f}{2} \frac{S^2}{\Theta} \left( 1 + \frac{S^2}{\Theta} \right). \quad (5)$$

Obviously, the solution of Eq. (2) coincides with the results

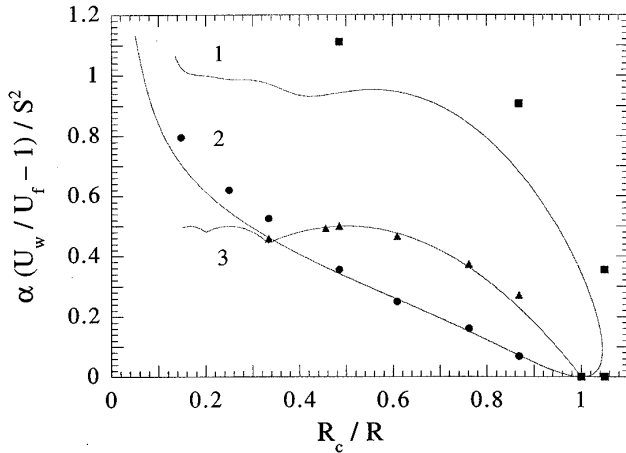


FIG. 1. The scaled flame velocity  $\alpha(U_w/U_f - 1)/S^2$  vs the inverse tube radius  $\delta = R_c/R$  for the convex flames (curve 1), concave flames (curve 2), and the 2D curved flames (curve 3). The markers show the results of numerical simulation of curved flames in tubes for  $\Theta = 5$ ; the squares, the circles, and the triangles correspond to the convex, concave, and 2D flames, respectively.

of 2D numerical simulations if one chooses the coefficient  $\alpha$  to be

$$\alpha = \frac{\Theta^2}{\Theta + S^2}. \quad (6)$$

Such a choice makes it possible to compare the results of Eq. (2) and the results of numerical simulations of flame dynamics for an arbitrary expansion coefficient.

In the present letter we use the modified nonlinear equation (2) to study the problem of axisymmetric curved three-dimensional (3D) flames propagating in cylindrical tubes. The configuration of a flame in a cylindrical tube is a common experimental situation (e.g., [3,13]), so that a curved flame with axial symmetry provides a typical example of a 3D curved flame. We obtain that the velocities of curved 3D flames are considerably larger than the corresponding velocities of 2D flames. We show that some important properties of the curved 3D flames are qualitatively different from the properties of 2D flames. Particularly, we obtain a regime of strong initiation of the LD instability in narrow tubes, when all perturbation modes of a small amplitude are stable, but a curved stationary flame is still possible. Another important point is the unlimited increase of the flame velocity with the increase of the tube diameter.

Let us consider propagation of a curved axisymmetric stationary flame  $f(\mathbf{x}, t) = F(r) - (U_w - U_f)t$  in a cylindrical tube of a radius  $R$  with ideally adiabatic walls. In this case the boundary conditions at the walls and at the tube axis become  $dF/dr = 0$  for  $r = 0, R$ . It is convenient to introduce the dimensionless variables and parameters  $W = \alpha S^{-2}(U_w - U_f)/U_f$ ,  $\varphi = \alpha F/(SR)$ ,  $\zeta = r/R$ ,  $\delta = R_c/R$ , where  $R_c = a_1 \lambda_c / 2\pi$  is the critical radius for which thermal conduction suppresses growth of small perturbations,  $a_1$  is the first of the roots  $a_n$  of the equation  $dJ_0(a)/da = 0$ ,  $J_0$  is the Bessel function of the zeroth order. For the introduced variables the nonlinear equation becomes

$$-W + \frac{1}{2} \left( \frac{d\varphi}{d\zeta} \right)^2 = \hat{I}(\varphi) + \frac{\delta}{a_1} \frac{1}{\zeta} \frac{d}{d\zeta} \left( \zeta \frac{d\varphi}{d\zeta} \right). \quad (7)$$

Because of the boundary conditions at the walls any solution of Eq. (7) may be presented as a sum of Bessel functions of zero order  $\varphi = \sum \varphi_n J_0(a_n \zeta)$ , so that the integral operator takes the form  $\hat{I}(\varphi) = \sum a_n \varphi_n J_0(a_n \zeta)$ . To find the latter formula one has to expand a planar wave  $\exp(i\mathbf{k} \cdot \mathbf{x})$  in terms of the Bessel functions and calculate the appropriate coefficients. However, an easier way to obtain the action of the operator  $\hat{I}$  on a Bessel function is to repeat the derivation [9] of Eq. (2) step by step, taking into account the cylindrical geometry from the very beginning.

Equation (7) has been solved numerically. For a function  $\varphi(\zeta)$  presented as a sum of Bessel harmonics the unknown amplitudes  $\varphi_n$  ( $n = 1, 2, \dots, N$ ) have to be found as an eigenvector of the eigenvalue problem with the eigenvalue  $W$ . The number  $N$  of the Bessel harmonics is determined by the accuracy requirements. The collocation technique [14] was used in order to obtain the equations for the coefficients  $\varphi_n$  and the scaled flame velocity  $W$ . Setting the right-hand side of Eq. (7) equal to the left-hand side in the collocation points  $\zeta_i = (2i - 1)/2(N + 1)$ ,  $i = 1, 2, \dots, N + 1$ , one obtains a system of algebraic equations for the unknown values  $W, \varphi_n$ . The system of algebraic equations has been solved by iterations. We start with  $\delta$  being close to unity and use the solution  $\varphi(\zeta) = \varphi_1 J_0(a_1 \zeta)$ ,  $W = \frac{1}{2} \varphi_1^2 J_0^2(a_1) a_1^2$  with

$$\varphi_1 = \frac{J_0^2(a_1)(1 - \delta)}{a_1 \int_0^1 J_0(a_1 \zeta) J_1^2(a_1 \zeta) \zeta d\zeta} \quad (8)$$

as an initial approximation. In order to find flame velocity for tubes of larger radius  $1 - \delta \sim 1$  the parameter  $\delta$  has been changed slowly. Solving Eq. (7) for any new parameter value  $\delta - \Delta \delta$  we took solution for the previous value  $\delta$  as an initial approximation. The convergency of the described numerical algorithm depends upon the problem parameter  $\delta$ : for narrow tubes  $|1 - \delta| \ll 1$  the convergency is rather good, while for wide tubes  $\delta = 0.1 - 0.2$  one has to take into account up to 80 modes to obtain reliable results.

Results of the numerical solution of Eq. (7) are presented in Figs. 1 and 2. The scaled velocity increase  $U_w/U_f - 1$  of a curved stationary flame in a cylindrical tube is shown in Fig. 1 versus the scaled inverse tube radius  $\delta = R_c/R$ . The velocity of a curved 2D flame in a tube with ideal walls Eqs. (4) and (5) is presented in Fig. 1 for comparison. It is seen from Fig. 1 that for the case of a cylindrical tube two solutions are possible with larger and smaller velocity increase. These solutions correspond to the configurations of a convex flame front (the solution with the larger velocity) and a concave flame front (the solution with the smaller velocity). The typical shapes of the concave and convex flames are shown in Fig. 2 for the parameter value  $\delta = 0.5$ . The velocity increase for a curved 3D flame is much larger than the velocity increase for a 2D flame. Particularly, for  $\delta = 0.5$  when the curved flame front results from the development of perturbations of a wavelength  $\lambda = 2\lambda_c$  the increase of the flame velocity for a convex 3D flame is almost doubled compared to the velocity increase of a 2D flame. For a flame in a gaseous fuel with expansion coefficients as large as  $\Theta = 10$  it implies that the velocity of a curved 3D flame may increase by quite a noticeable factor  $U_w \approx 1.7U_f$ .

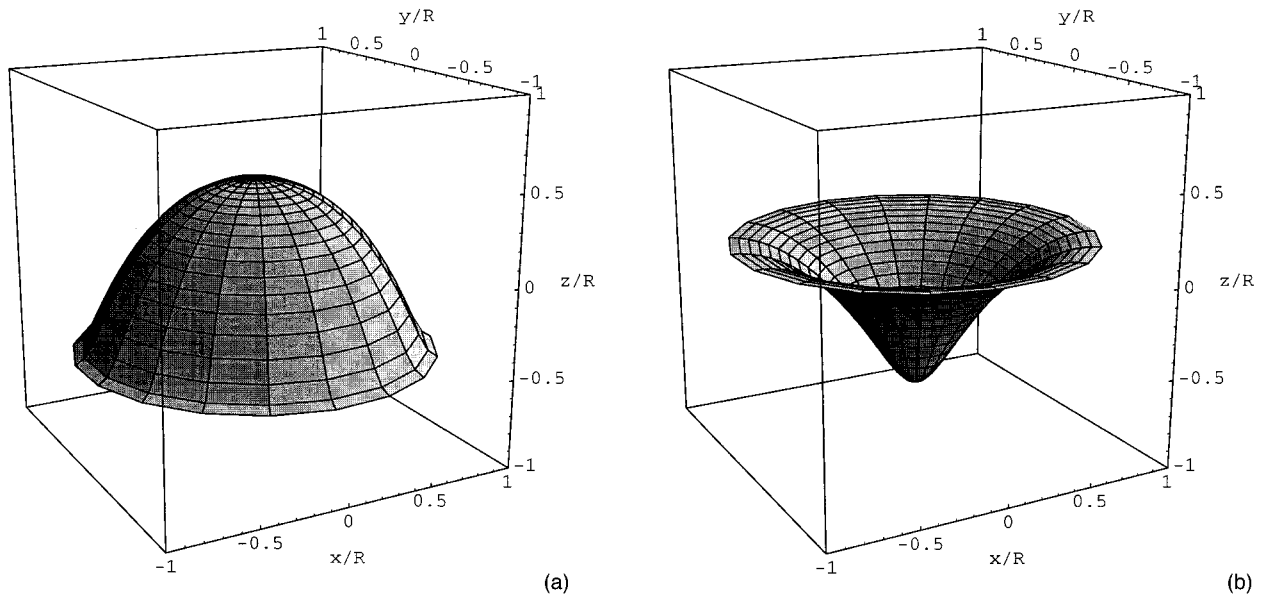


FIG. 2. The shapes of the convex (a) and concave (b) curved flames with cylindrical symmetry for the parameter value  $\delta = R_c/R = 0.55$ .

Figure 1 demonstrates that there are some features of 3D curved flames which are qualitatively different from that of 2D flames. One of them is the existence of curved axisymmetric stationary flames for narrow tubes  $R < R_c$  ( $\delta > 1$ ). For such a narrow tube all small perturbations of a planar flame front permitted by the boundary conditions at the tube walls belong to the stable domain of the dispersion relation Eq. (1). By this reason curved stationary flames obtained for  $\delta > 1$  may be interpreted as possibility of strong initiation of the LD instability in 3D configurations. Strong initiation implies that a flame front is stable against perturbations of an infinitesimal amplitude, while perturbations of some finite amplitude may grow with time and lead to the configuration of a curved stationary flame.

The dependence of the flame velocities on the tube radius is also quite different for the 2D and 3D curved flames. The difference is especially well pronounced for the concave 3D flame, which exhibits monotonous increase of the flame velocity with the increase of the tube radius. In this sense the dependence of the convex flame velocity on the tube radius presents some features of a 2D curved flame and some features of a concave flame. For tubes of moderate width the velocity dependence for the convex flame exhibits local maxima and minima like the velocity of a 2D curved flame. The points of maxima and minima of the convex flame velocity found numerically can be associated with the critical points of the Bessel function  $J_0$ :  $\delta = a_1/a_2 \approx 0.546$ ;  $\delta = a_1/a_3 \approx 0.376$ ;  $\delta = a_1/a_4 \approx 0.288$ , etc. For wide tubes the velocity of a convex flame increases monotonously with the tube radius similar to the concave flames. At the same time the increase of the flame velocity cannot be identified as the velocity increase expected for the fractal flames in wide tubes [15–17]: all calculated velocities correspond to smooth flame shapes with one hump or one cusp at the tube axis, while the fractal structure implies many cascades of humps and cusps of different sizes, imposed one on another.

Figure 1 shows the velocities of curved stationary axisymmetric flames with only one cusp or one hump when the first

Bessel harmonic is the principal one  $\varphi_1 \neq 0$ . For sufficiently wide tubes (sufficiently small  $\delta$ ) smooth solutions of Eq. (7) with  $\varphi_1 = 0$  are possible, which have several humps and cusps. Obviously, velocities of such solutions may be obtained from the velocity shown in Fig. 1 by the appropriate scaling of the  $\delta$  axis.

Since Eq. (2) is just a phenomenological extrapolation of a nonlinear equation derived in the peculiar limit of a small expansion coefficient  $\Theta - 1 \ll 1$  [9], one may doubt if the described properties of curved axisymmetric 3D flames are not just an artifact of the nonlinear model. To check this we performed numerical simulations of curved axisymmetric flames in cylindrical tubes for the complete set of the hydrodynamic equations of a reacting flow. The numerical code implements finite volume approximation of the hydrodynamical equations; see [5] for the details of the code and the numerical method. The numerical simulations of curved axisymmetric flames in cylindrical tubes support the physical results obtained on the basis of Eq. (2) (see Fig. 1). Thus, the solution of the generalized nonlinear equation (2) provides a good approximation for the flame velocity and may be helpful in complicated 3D configurations, when direct numerical simulations consume too much time.

Among the obtained properties of the curved 3D flames in cylindrical tubes the unlimited increase of the flame velocity with the increase of the tube radius is of special physical importance, since it implies that the flame velocity in wide tubes may become much larger than the velocity of the planar laminar flame. In a sense, it may be one of the explanations of the spontaneous flame acceleration and the detonation triggering by the accelerating flames in tubes, which has been observed many times in experiments [1].

This work was supported in part by the Swedish National Defense Research Establishment (FOA), by the Swedish National Board for Industrial and Technical Development (NUTEK), Grant No. P2204-2, by the Swedish Natural Science Research Council (NFR), Grant No. E-AD/EG 10297-316, and by the Swedish Royal Academy of Science.

- [1] Ya. B. Zel'dovich, G. I. Barenblatt, V. B. Librovich, and G. M. Makhviladze, *The Mathematical Theory of Combustion and Explosion* (Consultants Bureau, New York, 1985).
- [2] M. S. Uberoi, *Phys. Fluids* **2**, 72 (1959).
- [3] T. Maxworthy, *Phys. Fluids* **5**, 407 (1962).
- [4] B. Denet and P. Haldenwang, *Combust. Sci. Technol.* **104**, 143 (1995).
- [5] V. V. Bychkov, S. M. Golberg, M. A. Liberman, and L. E. Eriksson, *Phys. Rev. E* **54**, 3713 (1996).
- [6] P. Pelce and P. Clavin, *J. Fluid Mech.* **124**, 219 (1982).
- [7] M. Matalon and B. J. Matkowsky, *J. Fluid Mech.* **124**, 239 (1982).
- [8] M. A. Liberman, V. V. Bychkov, S. M. Golberg, and D. L. Book, *Phys. Rev. E* **49**, 445 (1994).
- [9] G. I. Sivashinsky, *Acta Astron.* **4**, 1177 (1977).
- [10] O. Thual, U. Frish, and M. Henon, *J. Phys. (France)* **46**, 1485 (1985).
- [11] S. Gutman and G. I. Sivashinsky, *Physica D* **43**, 129 (1990).
- [12] G. Joulin, *Phys. Rev. E* **50**, 2030 (1994).
- [13] C. Pelce-Savornin, J. Quinard, and G. Searby, *Combust. Sci. Technol.* **58**, 337 (1988).
- [14] C. A. J. Fletcher, *Computational Galerkin Methods* (Springer-Verlag, New York, 1984).
- [15] Y. A. Gostintsev, A. G. Istratov, and Y. V. Shulenin, *Combust. Explos. Shock Waves* **24**, 70 (1988).
- [16] S. I. Blinnikov and P. V. Sasorov, *Phys. Rev. E* **53**, 4827 (1996).
- [17] V. V. Bychkov and M. A. Liberman, *Phys. Rev. Lett.* **76**, 2814 (1996).